

Role of turnover in active stress generation in a filament network

Supplementary Material

Tetsuya Hiraiwa^{1,2,3} and Guillaume Salbreux^{1,4}

¹*Max Planck Institute for the Physics of Complex Systems, Nöthnitzerstraße 38, 01187 Dresden, Germany*

²*Fachbereich Physik, Freie Universität Berlin, Berlin, 14195, Germany*

³*Department of Physics, Graduate School of Science,*

The University of Tokyo, Tokyo, 113-0033, Japan

⁴*The Francis Crick Institute, 44 Lincoln's Inn Fields, London, WC2A 3LY, United Kingdom*

(Dated: April 27, 2016)

CALCULATION OF THE AVERAGE FORCE DIPOLE FOR TWO FILAMENTS

We detail here how we obtain the average force dipole exerted by a motor on two filaments in the configurations shown in Fig. 2. As mentioned in the text, we assume here that crosslinkers are rigidly fixed to the external network. The geometry of the two filaments and motor can be described by the positions of the motor on the two filaments s_1 , s_2 and by the two angles ψ_i between the motor filament and i -th filament ($i = 1, 2$). The motor positions s_i evolve according to

$$\mu \frac{ds_i}{dt} = -\frac{\partial U}{\partial s_i}, \quad (\text{S1})$$

while the angles ψ_i relax instantaneously, so that $\partial U / \partial \psi_i = 0$.

No crosslinkers attached, or one filament is attached by only one crosslinker and the other filament is rigidly attached to the external network

Case (i) and (iv): In these situations, no steady-state is reached as the motor always unbinds from the two filaments.

Two filaments attached to each other by a crosslinker

Case (ii): When the two filaments are attached to each other by a single crosslinker, the mechanical potential U reads

$$U = -f_0(x_1 + x_2) + \lambda \left(\sqrt{x_1^2 + x_2^2 - 2x_1x_2 \cos \theta} - l_m \right) \quad (\text{S2})$$

with x_1 and x_2 the distances between the myosin attachment points to the crossing point of the two filaments, taken positive in the direction of the filament towards which motors move (Fig. S1A). θ is the angle between the two filaments, such that $\mathbf{n}_1 \cdot \mathbf{n}_2 = \cos \theta$, with \mathbf{n}_i the unit vector giving the orientation of the filament i . In addition, λ is a Lagrange multiplier ensuring that the length l_m of the motor is fixed. Three situations can then occur:

- when $\theta \neq 0$ and $\theta \neq \pi$ and the filaments are not parallel neither antiparallel, the angle θ is given by

$$\cos \theta = \frac{x_1^2 + x_2^2 - l_m^2}{2x_1x_2} \quad (\text{S3})$$

and is free to adjust as the motor position changes. The evolution of the position of the motor on the filaments is given by

$$\mu \frac{dx_1}{dt} = f_0 \quad (\text{S4})$$

$$\mu \frac{dx_2}{dt} = f_0 \quad (\text{S5})$$

such that the motor moves until it detaches from the filaments, or until the filaments become parallel or antiparallel.

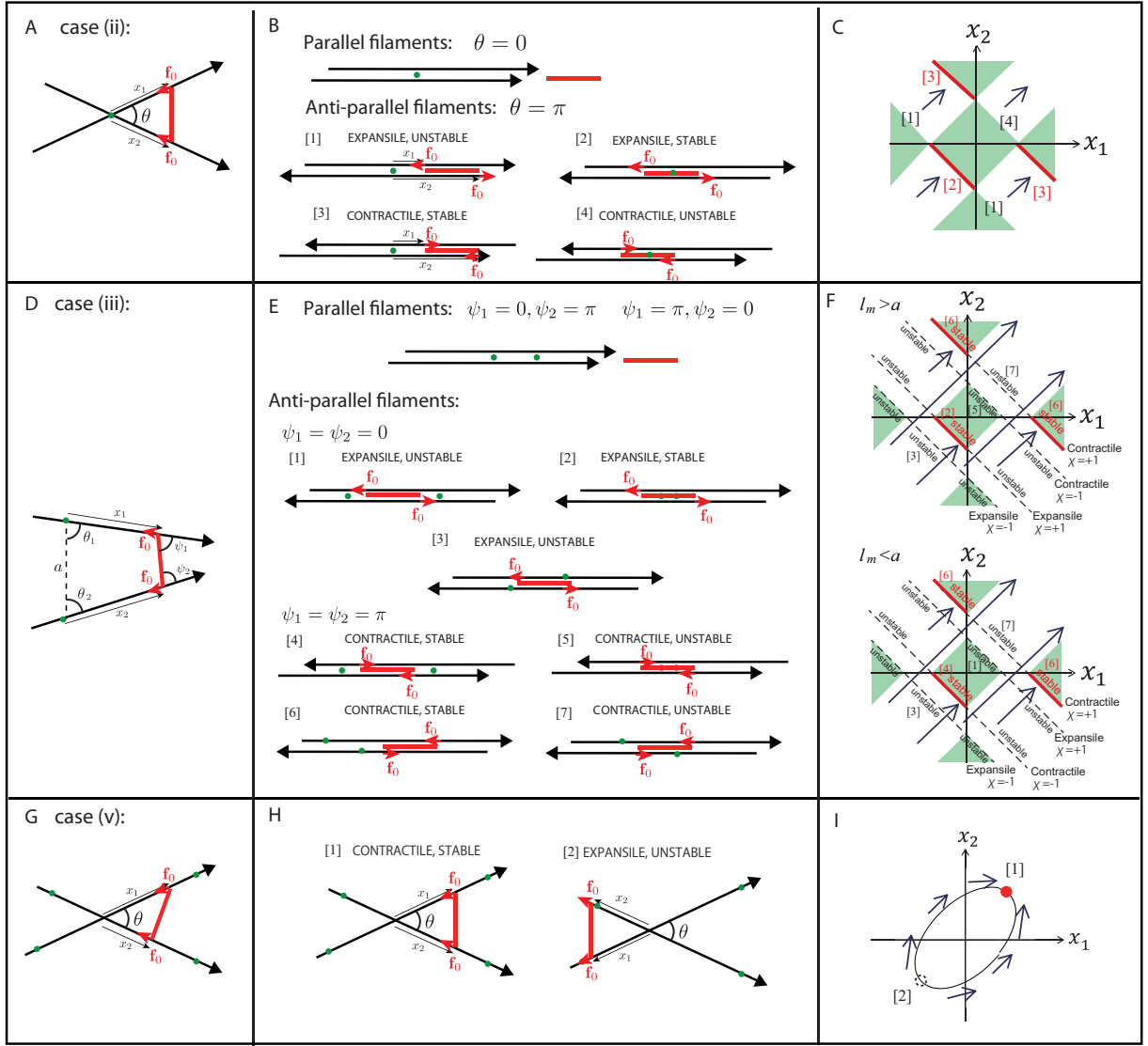


FIG. S1: Final configurations reached by two filaments bound by a motor, with the filaments attached to a rigid external network with a varying number of crosslinkers. A, D, G, example configurations for each case, according to the number of crosslinkers; B, E, H, corresponding possible steady-state configurations; C,F,I, Phase plot of the dynamics of the motor according to the coordinates of its position on the two filaments, x_1 , x_2 . Red lines and dots correspond to stable steady-state configurations, while dotted black lines correspond to unstable steady-state configurations. Green regions represent values of the coordinates x_1 and x_2 which are not geometrically accessible.

- When the two filaments are parallel and point in the same direction, $\theta = 0$ and $(x_1 - x_2)^2 = l_m^2$. The center of mass of the motor at position $(x_1 + x_2)/2$ follows the dynamic equation

$$\mu \frac{d}{dt} \frac{x_1 + x_2}{2} = f_0 \quad (S6)$$

and the motor moves on the filament until it detaches.

- When the two filaments are antiparallel, $\theta = \pi$ and $(x_1 + x_2)^2 = l_m^2$. Two configurations are then possible, according to whether the two filaments point away or towards the center of the motor from their attachment point to the motor. These two configurations correspond respectively to $x_1 + x_2 = -l_m$ (expansile configuration) and $x_1 + x_2 = l_m$ (contractile configuration). Any position of the motor on the filament is then a steady-state solution, as long as the two motor ends each bind on the filaments.

To test for the stability of these two configurations, we consider a slight change of the angle between the two filaments, $\theta = \pi + \delta\theta$, with $|\delta\theta| \ll 1$. We take the initial position of the motor to be $x_1 = x_0 + \chi l_m/2$ and

$x_2 = -x_0 + \chi l_m/2$, with $\chi = -1$ for an expansile configuration and $\chi = 1$ for a contractile configuration. $x_0 = (x_1 - x_2)/2$ is the position of the center of mass of the motor, relative to the crosslinker joining the two filaments, measured positively in the direction of the first filament. We find then the following dynamic equation for $\delta\theta$:

$$\begin{aligned} \mu \frac{d\delta\theta}{dt} &= \mu \left[\frac{dx_1}{dt} \frac{\partial\theta}{\partial x_1} + \frac{dx_2}{dt} \frac{\partial\theta}{\partial x_2} \right] \\ &= f_0 \frac{8\chi l_m}{l_m^2 - 4x_0^2} \frac{1}{\delta\theta} \end{aligned} \quad (\text{S7})$$

where we have used Eqs. (S3), (S4) and (S5) from the first to the second line. The sign of the right hand side of Eq. (S7) indicates whether the angle θ increases or decreases when the two filaments are slightly rotated away from their antiparallel configuration. Therefore, the associated configuration is unstable when the sign is positive, and stable otherwise. We find therefore that the stability of the configuration depends on the position of the center of mass of the motor: for $|x_0| < l_m/2$ (motor near the crosslinker), the expansile configuration is stable, and the contractile configuration unstable. For $|x_0| > l_m/2$ (motor away from the crosslinker), the expansile configuration is unstable and the contractile configuration is stable.

The flow diagram in Fig. S1C shows the corresponding dynamics in the space of the motor position (x_1, x_2) . Red segments indicate the stable steady states. In the green regions, no value of the angle θ allows for the motor to have position (x_1, x_2) on the two filaments.

Two filaments, each attached by a crosslinker to the external network

The mechanical potential reads in that case

$$U = -f_0(x_1 + x_2) + \lambda \left[\sqrt{x_1^2 + x_2^2 + l_m^2 + 2x_1 l_m \cos \psi_1 + 2x_2 l_m \cos \psi_2 + 2x_1 x_2 \cos(\psi_1 + \psi_2)} - a \right], \quad (\text{S8})$$

with x_1 and x_2 the distances between the myosin attachment point and the crosslinker position on each filament, and $a \neq 0$ the distance between the two crosslinkers (Fig. S1D). λ is a Lagrange multiplier imposing that the length of the motor is equal to l_m . In this subsection, we use for convenience the dynamics of the angle between motor and filaments ψ_1 and ψ_2 to characterise the orientation of the filaments. The dynamics in the limit where the relaxation of ψ_1 and ψ_2 is taken into account is given by

$$\mu \frac{dx_1}{dt} = f_0 - \frac{\lambda}{a} (x_1 + l_m \cos \psi_1 + x_2 \cos(\psi_1 + \psi_2)) \quad (\text{S9})$$

$$\mu \frac{dx_2}{dt} = f_0 - \frac{\lambda}{a} (x_2 + l_m \cos \psi_2 + x_1 \cos(\psi_1 + \psi_2)) \quad (\text{S10})$$

$$\epsilon \mu a^2 \frac{d\psi_1}{dt} = \frac{\lambda}{a} (x_1 l_m \sin \psi_1 + x_1 x_2 \sin(\psi_1 + \psi_2)) \quad (\text{S11})$$

$$\epsilon \mu a^2 \frac{d\psi_2}{dt} = \frac{\lambda}{a} (x_2 l_m \sin \psi_2 + x_1 x_2 \sin(\psi_1 + \psi_2)) \quad (\text{S12})$$

where $\epsilon \ll 1$ is a factor that vanishes in the quasi-static limit where the filaments rotate adiabatically. Solving for the Lagrange multiplier λ by imposing the constraint that the length of the motor is equal to l_m , we obtain:

$$\lambda = \epsilon f_0 a^3 \frac{(x_1 + x_2)(1 + \cos(\psi_1 + \psi_2)) + l_m(\cos \psi_1 + \cos \psi_2)}{A + B\epsilon a^2} \quad (\text{S13})$$

$$A = (x_1 l_m \sin \psi_1 + x_1 x_2 \sin(\psi_1 + \psi_2))^2 + (x_2 l_m \sin \psi_2 + x_1 x_2 \sin(\psi_1 + \psi_2))^2$$

$$B = (x_1 + l_m \cos \psi_1 + x_2 \cos(\psi_1 + \psi_2))^2 + (x_2 + l_m \cos \psi_2 + x_1 \cos(\psi_1 + \psi_2))^2$$

where the coefficient A vanishes when the filaments are aligned with the motor. Several situations can again be distinguished:

- When the filaments are neither parallel nor antiparallel, from Eq. (S13), $\lambda \sim \epsilon$ in the limit $\epsilon \rightarrow 0$. Eqs. (S9) and (S10) then yield at the lowest order in ϵ

$$\mu \frac{dx_1}{dt} = f_0 + O(\epsilon) \quad (\text{S14})$$

$$\mu \frac{dx_2}{dt} = f_0 + O(\epsilon) \quad (\text{S15})$$

such that no steady-state exists in that situation.

- When the filaments are parallel and point in the same direction, $(\psi_1, \psi_2) = (0, \pi)$ or $(\psi_1, \psi_2) = (\pi, 0)$. In that case $\lambda = 0$ and no steady-state exists for the motor, which runs on the two filaments before detachment.
- When the filaments are antiparallel, $(\psi_1, \psi_2) = (0, 0)$ (expansile configuration) or $(\psi_1, \psi_2) = (\pi, \pi)$ (contractile configuration). In the expansile configuration, $x_1 + x_2 + l_m = \chi a$, with $\chi = \pm 1$. In the contractile configuration, $x_1 + x_2 - l_m = \chi a$, with the same rule applying for χ . In both cases, Eq. (S13) yields $\lambda = \chi f_0$ and any position of the motor is a steady-state.

To test for the stability of these steady states, we consider the dynamics of ψ_1 and ψ_2 around $\psi_1 = \psi_2 = \psi^*$ with $\psi^* \equiv 0$ or π . We write therefore $\psi_1 = \psi^* + \delta\psi_1$ and $\psi_2 = \psi^* + \delta\psi_2$. To regularise the dynamics around the parallel filaments state, we consider a situation with non-zero ϵ and consider perturbations verifying $\delta\psi \ll \sqrt{\epsilon}$, such that $\lambda \simeq \chi f_0$. From Eqs. (S11) and (S12), we have then

$$\epsilon \mu a^2 \frac{d\delta\psi_1}{dt} = \frac{\chi f_0}{a} [(x_1 l_m \cos \psi^* + x_1 x_2) \delta\psi_1 + x_1 x_2 \delta\psi_2] \quad (\text{S16})$$

$$\epsilon \mu a^2 \frac{d\delta\psi_2}{dt} = \frac{\chi f_0}{a} [x_1 x_2 \delta\psi_1 + (x_2 l_m \cos \psi^* + x_1 x_2) \delta\psi_2], \quad (\text{S17})$$

so that the state $\psi_1 = \psi_2 = \psi^*$ is stable if $\chi(x_1 l_m \cos \psi^* + x_2 l_m \cos \psi^* + 2x_1 x_2) < 0$ and $(x_1 l_m \cos \psi^* + x_1 x_2)(x_2 l_m \cos \psi^* + x_1 x_2) - x_1^2 x_2^2 > 0$, whereas it is unstable otherwise. Taking the initial condition to be $x_1 = x_0/2 + (\chi a - l_m \cos \psi^*)/2$ and $x_2 = -x_0/2 + (\chi a - l_m \cos \psi^*)/2$ at the steady state, the stability condition is satisfied when

$$\chi(x_0^2 + l_m^2 - a^2) > 0 \text{ and } x_1 x_2 \chi \cos \psi^* > 0. \quad (\text{S18})$$

The results are summarized in the flow diagram in Fig. S1F. Red segments indicate the stable steady states. In the green region, there are no possible values of ψ_1 and ψ_2 for given values of x_1 and x_2 .

Two filaments rigidly attached to the external network

This situation corresponds to case (v). The mechanical potential U reads as for case (ii)

$$U = -f_0(x_1 + x_2) + \lambda \left(\sqrt{x_1^2 + x_2^2 - 2x_1 x_2 \cos \theta} - l_m \right), \quad (\text{S19})$$

with x_1 and x_2 the distances to the crossing point of the two filaments, taken positive in the direction of the filament towards which motors move (Fig. S1G). θ is the angle between the two filaments, such that $\mathbf{n}_1 \cdot \mathbf{n}_2 = \cos \theta$, with \mathbf{n}_i the unit vector giving the orientation of the filament i . λ is a Lagrange multiplier ensuring that the length l_m of the motor is fixed. The dynamic equation for the motion of the motor on the two filaments Eq. (S1) then reads

$$\mu \frac{dx_1}{dt} = f_0 - \frac{\lambda}{l_m} (x_1 - x_2 \cos \theta) \quad (\text{S20})$$

$$\mu \frac{dx_2}{dt} = f_0 - \frac{\lambda}{l_m} (x_2 - x_1 \cos \theta), \quad (\text{S21})$$

where θ is a fixed angle, and the Lagrange multiplier λ is obtained from the constraint that $x_1^2 + x_2^2 - 2x_1 x_2 \cos \theta = l_m^2$:

$$\lambda = \frac{f_0 l_m (x_1 + x_2) (1 - \cos \theta)}{(x_1 - x_2 \cos \theta)^2 + (x_2 - x_1 \cos \theta)^2} \quad (\text{S22})$$

Two solutions can be found for the motor position on the two filaments, assuming that they are not parallel ($\theta \neq 0$ and $\theta \neq \pi$):

$$x_1 = x_2 = \pm \frac{l_m}{2 \sin \frac{\theta}{2}} \quad (\text{S23})$$

As pointed out in Ref. [1], a linear stability analysis around the steady-state indicates that only the positive solutions $x_1 = x_2 = l_m/[2|\sin(\theta/2)|]$ is stable. The corresponding force dipole at equilibrium is positive and is given by

$$d = \frac{l_m f_0}{|\sin(\frac{\theta}{2})|}. \quad (\text{S24})$$

Therefore, the dipole formed on two rigidly fixed, non-parallel filaments is always contractile (Fig. S1H-I).

Average force dipoles

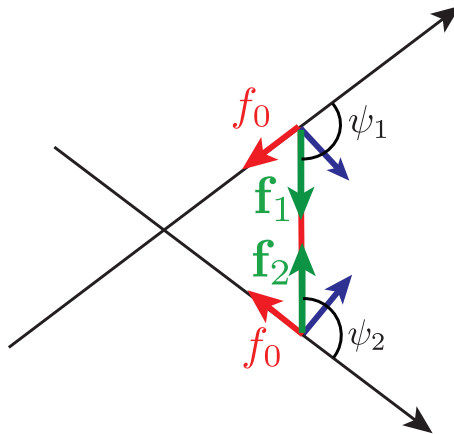


FIG. S2: Schematic of the force dipole exerted by a motor. Each motor exerts a force of magnitude f_0 parallel to the filament. The total force exerted by the motor on the filament are equal and opposite at steady-state and denoted \mathbf{f}_1 and \mathbf{f}_2 . The contribution of the force normal to the filament arises from geometrical constraints. Overall, this results in a tension $f = |\mathbf{f}_1| = |\mathbf{f}_2|$ acting within the motor, which is used here to define the force dipole exerted by a motor.

To obtain the associated average force dipole exerted by the motor in these different configurations, we proceed as follows: denoting as $\mathbf{c}_{12}^{(0)}$ the initial distance between the two filaments, $\theta_{f,1}^{(0)}$ and $\theta_{f,2}^{(0)}$ the two angles giving the initial orientations of the filaments, $x_{m,1}^{(0)}$, $x_{m,2}^{(0)}$ the initial position of the two motors on the filaments, and r_k ($k = 1, \dots, N_c$ with N_c the number of crosslinkers attached to the external network) the position of the crosslinkers on the filaments, we compute the motor-induced force dipole d reached at steady-state as shown in Fig. S2 by

$$d(\mathbf{c}_{12}^{(0)}, \theta_{f,1}^{(0)}, \theta_{f,2}^{(0)}, x_{m,1}^{(0)}, x_{m,2}^{(0)}, \{r_k\}_k) = -\frac{l_m f_0}{2 \cos \psi_1} - \frac{l_m f_0}{2 \cos \psi_2}, \quad (\text{S25})$$

where the angles ψ_1 and ψ_2 between the motor and two filaments at steady-state are functions of $\mathbf{c}_{12}^{(0)}$, $\theta_{f,1}^{(0)}$, $\theta_{f,2}^{(0)}$, $x_{m,1}^{(0)}$, $x_{m,2}^{(0)}$ and $\{r_k\}_k$. Equation (S25) is obtained from the definition of the force dipole

$$d = \frac{l_m}{2} \mathbf{n}_{12} \cdot (\mathbf{f}_1 - \mathbf{f}_2) \quad (\text{S26})$$

with \mathbf{n}_{12} the unit vector giving the motor orientation pointing from filament 1 to filament 2, and \mathbf{f}_i with $i = 1, 2$ are the forces exerted by the motor on the two filaments. The dependencies $-1/\cos \psi_i$ ($i = 1, 2$) in Eq. (S25) arise from the condition that the projections of the forces \mathbf{f}_i on the filament i have magnitude f_0 (Fig. S2).

The average force dipole is then obtained by

$$\langle d \rangle = \frac{1}{\Gamma} \int d\mathbf{c}_{12}^{(0)} \int_0^{2\pi} d\theta_{f,2}^{(0)} \int_0^{2\pi} d\theta_{f,1}^{(0)} \int \left(\prod_{k=1}^{N_c} dr_k \right) \int d\{x_{m,1}^{(0)}, x_{m,2}^{(0)}\} d(\mathbf{c}_{12}^{(0)}, \theta_{f,1}^{(0)}, \theta_{f,2}^{(0)}, x_{m,1}^{(0)}, x_{m,2}^{(0)}, \{r_k\}_k), \quad (\text{S27})$$

where the integration $\int d\{x_{m,1}^{(0)}, x_{m,2}^{(0)}\}$ runs for all possible initial motor configurations $x_{m,1}^{(0)}, x_{m,2}^{(0)}$ that eventually reach a steady state, and $\Gamma = \int d\mathbf{c}_{12}^{(0)} \int d\{x_{m,1}^{(0)}, x_{m,2}^{(0)}\} (2\pi)^2 (L_f)^{N_c}$.

RELATIONSHIP BETWEEN THE STRESS AND THE AVERAGE FORCE DIPOLE

In this section, we discuss the two contributions to the stress generated by the filament and motor network, σ_{ij}^f and σ_{ij}^m . We point out that in the absence of large scale deformations, σ_{ij}^f can contribute to the total stress, when the elastic response of the filament network is non-linear.

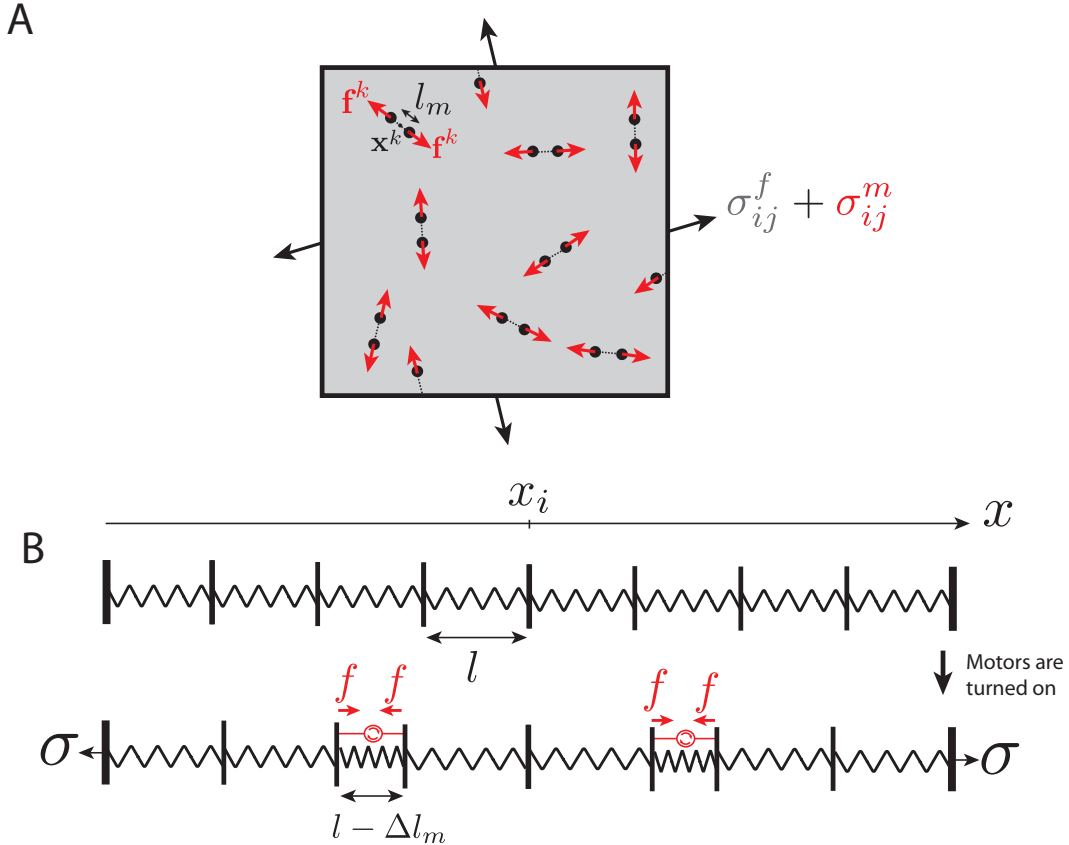


FIG. S3: A. Schematic of a 2D elastic material, subjected to forces arising from force dipoles exerted by motor filaments. Motors result in a stress σ_{ij} acting at the boundary of the box. B. Schematic of a 1D chain of non linear springs subjected to force dipoles. The chain contains N springs and is fixed at both ends. Motors result in a force σ along the chain.

Two-dimensional, linear elastic material

We consider here a two-dimensional elastic material subjected to the force dipoles exerted by motor filaments. The motor force dipoles consist of two opposite forces $\mathbf{f}^k = \pm f^k \mathbf{n}^k$, separated by a distance l_m , and where the index k label the motors. The motors induce a deformation in the elastic material. The total stress in the system is then the sum of the resulting elastic stress, denoted σ_{ij}^f , and the stress generated within the motors, denoted σ_{ij}^m :

$$\sigma_{ij} = \sigma_{ij}^f + \sigma_{ij}^m \quad (\text{S28})$$

We start by discussing the average stress created by an ensemble of motors in a 2D material. Following Ref. [2], we now show that when the system is homogeneous, force balance on a section \mathcal{S} of the network enclosed in a contour \mathcal{C} allows to relate the stress generated within motors to the concentration and orientation of motors. To evaluate the

stress, we first note that each motor k corresponds to a line under tension f^k with length l_m , orientation \mathbf{n}^k , centered at position \mathbf{x}^k , and joining the two points at coordinates $\mathbf{x}^k - l_m/2\mathbf{n}^k$ and $\mathbf{x}^k + l_m/2\mathbf{n}^k$ (Fig. S3A). Therefore, the two-dimensional stress field within the motors can be written

$$\sigma_{ij}^m(\mathbf{x}) = \sum_k f^k n_i^k n_j^k \int_{-\frac{l_m}{2}}^{\frac{l_m}{2}} du \delta(\mathbf{x} - (\mathbf{x}^k + \mathbf{n}^k u)) \quad (\text{S29})$$

where u is a coordinate going along the line under tension f^k . The average stress within a region \mathcal{S} of surface area S is then given by

$$\langle \sigma_{ij}^m \rangle = \frac{1}{S} \int_{\mathcal{S}} d\mathbf{x} \sigma_{ij}^m(\mathbf{x}) \quad (\text{S30})$$

$$= \frac{1}{S} \int_{\mathcal{S}} d\mathbf{x} \sum_k f^k n_i^k n_j^k \int_{-\frac{l_m}{2}}^{\frac{l_m}{2}} du \delta(\mathbf{x} - (\mathbf{x}^k + \mathbf{n}^k u)) \quad (\text{S31})$$

$$= \frac{1}{S} \sum_k f^k l_m n_i^k n_j^k \quad (\text{S32})$$

$$= c \langle dn_i n_j \rangle \quad (\text{S33})$$

where c is the concentration of motors, $d^k = l_m f^k$ is the dipole strength of motor k , and the averaging $\langle \cdot \rangle$ is performed over space.

In a linearly elastic material, the average stress within the network of filaments is given by

$$\sigma_{ij}^f = 2E \left(u_{ij} - \frac{1}{2} u_{kk} \delta_{ij} \right) + K u_{kk} \delta_{ij} \quad (\text{S34})$$

with E and K a shear and bulk elastic moduli, and $u_{ij} = \frac{1}{2}(\partial_i u_j + \partial_j u_i)$ the gradient of deformation. The average stress generated in the elastic material in a region \mathcal{S} with contour \mathcal{C} and surface area S is then given by

$$\langle \sigma_{ij}^f \rangle = \frac{1}{S} \int_{\mathcal{S}} d\mathbf{x} \sigma_{ij}^f \quad (\text{S35})$$

$$= \frac{2E}{S} \int_{\mathcal{S}} d\mathbf{x} u_{ij} + \frac{K-E}{S} \int_{\mathcal{S}} d\mathbf{x} u_{kk} \delta_{ij} \quad (\text{S36})$$

$$= \frac{E}{S} \int_{\mathcal{C}} dl \nu_i u_j + \frac{E}{S} \int_{\mathcal{C}} dl \nu_j u_i + \frac{K-E}{S} \int_{\mathcal{C}} dl \nu_k u_k \delta_{ij} \quad (\text{S37})$$

where $\boldsymbol{\nu}$ is the vector normal to the contour \mathcal{C} and dl an infinitesimal line element on the contour. If we consider a square box whose boundaries are fixed (Fig. S3A), or periodic boundary conditions, the contour integrals in Eq. (S37) vanish. Therefore, for a linear elastic material with fixed boundaries, the average stress arises entirely from the forces acting within the motors. This however does not apply to a non-linearly elastic material, as we show in the next section.

One-dimensional chain of non-linear springs

We consider a simpler example in 1D of a periodic chain of N elastic springs. Each spring is located between positions x_i and x_{i+1} , with initial resting position $x_i = il$. The two points at the end of the chain, x_0 and x_N , are not allowed to move. In addition, N_m motors are acting in parallel to a fraction $n = N_m/N$ of the springs (Fig. S3B). The motor exerts a constant force f . The springs have a non-linear force-extension relation

$$f_e = k \frac{\Delta l}{l} + k_2 \left(\frac{\Delta l}{l} \right)^2 \quad (\text{S38})$$

with f_e the force exerted by the spring, $\Delta l = x_{i+1} - x_i - l$ the extension of the spring, and k and k_2 are two spring constants. We assume that the springs are weakly non-linear, $k_2/k \ll 1$. In the initial resting position, $\Delta l = 0$. The motors are then turned-on, driving a deformation of the the springs in the chain. The contraction of the springs which are in parallel with the motors is denoted $-\Delta l_m$. Because the overall length of the chain is kept fixed, the

deformation of the free springs is then given by $\Delta l_m n / (1 - n)$. We denote by σ the total force acting within the chain. Force balance imposes that the total force within the springs and the motors is fixed and equal to σ , giving

$$\sigma = -k \frac{\Delta l_m}{l} + k_2 \left(\frac{\Delta l_m}{l} \right)^2 + f = k \frac{\Delta l_m}{l} \frac{n}{1 - n} + k_2 \left(\frac{\Delta l_m}{l} \frac{n}{1 - n} \right)^2 \quad (\text{S39})$$

where the second part of the equality is the total force within the springs in parallel with a motor, and the third part the force within the free springs. Solving these equations and expanding to first order in $f k_2 / k^2 \ll 1$, one obtains

$$\sigma = f n + \frac{k_2 f^2 n (1 - n)}{k^2} \quad (\text{S40})$$

or using the concentration of motors $c = n/l$,

$$\sigma = f l c + \frac{k_2 f^2}{k^2} c l (1 - c l) \quad (\text{S41})$$

$$= \sigma^m + \sigma^f \quad (\text{S42})$$

where $\sigma^m = f l c$ is the average tension exerted within the motors. To leading order in the spring non linearity, $k_2 \rightarrow 0$, the force within the chain reduces to the average motor tension σ^m , in agreement with Eq. (S33). The non-linear elastic behaviour however brings a correction to this term $\sigma^f = k_2 f^2 c l (1 - c l) / k^2$, proportional to the motor force squared, f^2 .

NETWORK RELAXATION TIME

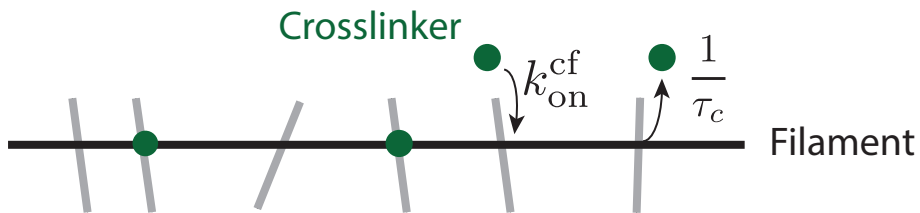


FIG. S4: Schematic of a filament in the network. Crosslinkers bind to the filament with rate k_{on}^{cf} and unbind with rate $1/\tau_c$.

We derive here an approximate expression for the network characteristic relaxation time. We consider a filament within the network, crossing other filaments that are themselves immobilised. We expect this last assumption to be valid for a large enough number of crosslinkers. The number of crossing points is assumed to largely exceed the total number of crosslinkers in the network. Crosslinkers bind and unbind the filament at crossing points with other filaments. A filament with two attached crosslinkers is completely fixed, and can only rotate when it has one attached crosslinker. For simplicity we consider here that the filament can not rearrange to relax stresses unless no crosslinker attaches it to other filaments in the network. Once a filament is free, it can move until a crosslinker binds to it and immobilise it. We therefore estimate the network relaxation time as the mean first passage time to a state where no crosslinkers bind the filament, from a state where one crosslinker binds the filament.

We consider the probability of having n_c crosslinkers on the filament, $P(n_c)$. New crosslinkers bind to the filament with rate $k_{on}^{cf} = 2[k_{on}^c / (1 + k_{on}^c \tau_c)] N_c / N_f$, as crosslinkers bind to all filaments in the network with rate k_{on}^c (Fig. S4), and each crosslinker binds two filaments. In addition, crosslinkers unbind from the filament with rate τ_c^{-1} (Fig. S4). The probability $P(n_c)$ then follows the master equation:

$$\frac{dP(n_c)}{dt} = \frac{n_c + 1}{\tau_c} P(n_c + 1) + k_{on}^{cf} P(n_c - 1) - \left(\frac{n_c}{\tau_c} + k_{on}^{cf} \right) P(n_c) \quad (\text{S43})$$

Stationary distribution. The stationary distribution of Eq. (S43) is a Poisson distribution:

$$P(n_c) = e^{-k_{on}^{cf} \tau_c} \frac{(k_{on}^{cf} \tau_c)^{n_c}}{n_c!} \quad (\text{S44})$$

with mean and variance $n_c^* = k_{on}^{cf} \tau_c \simeq 2N_c / N_f$ for $k_{on}^c \tau_c \gg 1$.

Mean first passage time. We now want to obtain the mean first passage time to reach a state where the filament has no bound crosslinker, $n_c = 0$, starting from a configuration with n crosslinkers attached on the filament. We denote T_n this first passage time, and we follow a standard procedure to obtain its value [3, 4]. T_n satisfies the following equation for $n > 0$:

$$T_n = \frac{k_{on}^{cf}}{k_{on}^{cf} + n/\tau_c} T_{n+1} + \frac{n/\tau_c}{k_{on}^{cf} + n/\tau_c} T_{n-1} + \frac{1}{k_{on}^{cf} + n/\tau_c} \quad (\text{S45})$$

where the first term corresponds to the probability of moving to a state with $n + 1$ bound crosslinkers, times the waiting time from the state $n + 1$, the second term is the product of the probability to move to a state with $n - 1$ bound crosslinkers times the waiting time from the state $n - 1$, and the last term is the average time spent in the state n . In addition, $T_0 = 0$ by definition of the first passage time T_n , and we take a reflecting boundary condition at infinity, implying $T_n - T_{n-1} \rightarrow 0$ for $n \rightarrow \infty$. Equation (S45) can be rewritten

$$k_{on}^{cf}(T_n - T_{n+1}) + \frac{n}{\tau_c}(T_n - T_{n-1}) = 1 \quad (\text{S46})$$

or defining $z_n = T_{n+1} - T_n$,

$$z_n = \frac{n}{k_{on}^{cf}\tau_c} z_{n-1} - \frac{1}{k_{on}^{cf}} \quad (\text{S47})$$

To solve this equation, one introduces $Z_n = z_n(k_{on}^{cf}\tau_c)^n/n!$, which satisfies then:

$$Z_n = Z_{n-1} - \frac{(k_{on}^{cf}\tau_c)^n}{k_{on}^{cf}n!} \quad (\text{S48})$$

Solving Eq. (S48) then yields the following expression for Z_n , z_n and T_n , using that $Z_\infty = 0$:

$$Z_n = \sum_{k=n+1}^{\infty} \frac{(k_{on}^{cf}\tau_c)^k}{k_{on}^{cf}k!} \quad (\text{S49})$$

$$z_n = \frac{n!}{(k_{on}^{cf}\tau_c)^n} \sum_{k=n+1}^{\infty} \frac{(k_{on}^{cf}\tau_c)^k}{k_{on}^{cf}k!} \quad (\text{S50})$$

$$T_n = \sum_{k=0}^{n-1} \frac{k!}{(k_{on}^{cf}\tau_c)^k} \sum_{m=k+1}^{\infty} \frac{(k_{on}^{cf}\tau_c)^m}{k_{on}^{cf}m!} \quad (\text{S51})$$

From this last expression, one finally obtains T_1 ,

$$T_1 = \sum_{m=1}^{\infty} \frac{(k_{on}^{cf}\tau_c)^m}{k_{on}^{cf}m!} \quad (\text{S52})$$

$$= \frac{1}{k_{on}^{cf}} (e^{k_{on}^{cf}\tau_c} - 1) \quad (\text{S53})$$

$$= \frac{\tau_c}{n_c^*} (e^{n_c^*} - 1) \quad (\text{S54})$$

The time T_1 therefore contains a factor increasing exponentially with the number of crosslinkers per filament n_c^* . We use the time T_1 as an estimate for the network relaxation time. In Fig. 3f, we verify that the time T_1 provides a good approximation for the relaxation time of the network.

EFFECT OF MOTOR CONCENTRATION AND DISPERSION IN MOTOR FORCES

We have performed additional simulations measuring the isotropic stress σ as the concentration of myosin motors N_m/W^2 is varied (Figure. S5A). The reference stress σ_0 is defined as being proportional to motor concentration, such that $\sigma \sim \sigma_0$ indicates that the stress is proportional to the myosin concentration. We find that σ has a weak non-linear dependence as a function of the myosin number N_m for the simulation parameters plotted in Figure S5A,

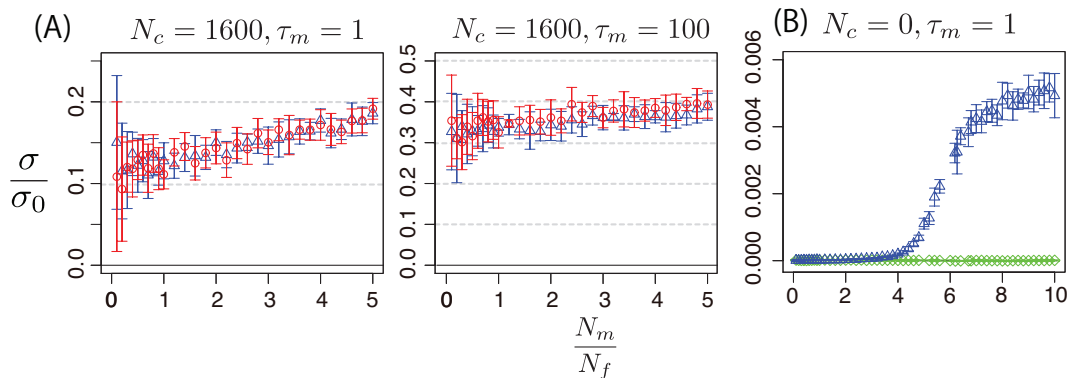


FIG. S5: A. Isotropic stress as a function of the number of motors N_m , for two values of myosin turnover. In these graphs, we performed the simulations for the cases with identical motors (red circles) and with a dispersion of 20% motor force and friction (blue triangles). Non-specified parameters are as in Fig. 3 of the main text. B. Isotropic stress as a function of the number of motors, in the absence of a crosslinker. Green diamond marks, identical motors; no stress is generated. Blue triangle marks, a dispersion of 20% motor force and friction results in a non-zero stress for a high enough number of motors. Non-specified parameters are as in Fig. 3 of the main text. Stress was averaged here over 10τ after initialization.

and is nearly linearly increasing with N_m for slow enough turnover. This indicates that the stress generated by the simulated network is roughly proportional to the myosin concentration.

In our simulations, motors are identical and have the same stall force; as a result no stress is generated in the absence of crosslinkers (Fig. 3 and Ref [5]). Introducing a dispersion in motor friction and stall force however can result in stress generation as the number of myosin motors is increased (Figure. S5B). The overall stress generated is much smaller than stresses generated for the same parameters with a cross linked network.

SUPPLEMENTARY MOVIE LEGENDS

- *Supp. Movie M1* Simulation of a network with no crosslinker turnover, no filament turnover, $N_c = 800$ and $\tau_m = 100\tau$. Total simulation time, 1600τ . The number of crosslinkers N_c is below the threshold for the network to exert a contractile stress.
- *Supp. Movie M2* Simulation of a network with no crosslinker turnover, no filament turnover, $N_c = 1100$ and $\tau_m = 100\tau$. Total simulation time, 1600τ . The number of crosslinkers N_c is above the threshold for the network to exert a contractile stress.
- *Supp. Movie M3* Simulation of a network with no filament turnover, crosslinker turnover with $\tau_c = 100\tau$, $N_c = 1200$ and $\tau_m = 100\tau$. Total simulation time, 1600τ . The network collapses and does not exert a contractile stress in steady state.
- *Supp. Movie M4* Simulation of a network with filament turnover with $\tau_a = 100\tau$, crosslinker turnover with $\tau_c = 100\tau$, $N_c = 800$ and $\tau_m = 100\tau$. Total simulation time, 1600τ . The network reaches a steady-state where no contractile stress is exerted.
- *Supp. Movie M5* Simulation of a network with filament turnover with $\tau_a = 100\tau$, crosslinker turnover with $\tau_c = 100\tau$, $N_c = 1200$ and $\tau_m = 100\tau$. Total simulation time, 1600τ . The network reaches a steady-state where a contractile stress is exerted.

-
- [1] Nilushi L Dasanayake, Paul J Michalski, and Anders E Carlsson. General mechanism of actomyosin contractility. *Physical review letters*, 107(11):118101, 2011.
- [2] R Aditi Simha and Sriram Ramaswamy. Hydrodynamic fluctuations and instabilities in ordered suspensions of self-propelled particles. *Physical review letters*, 89(5):058101.1–058101.4, 2002.
- [3] CW Gardiner. *Stochastic methods*. Springer-Verlag, Berlin–Heidelberg–New York–Tokyo, 1985.

- [4] Pedro A Pury and Manuel O Cáceres. Mean first-passage and residence times of random walks on asymmetric disordered chains. *Journal of Physics A: Mathematical and General*, 36(11):2695, 2003.
- [5] Martin Lenz, Margaret L Gardel, and Aaron R Dinner. Requirements for contractility in disordered cytoskeletal bundles. *New journal of physics*, 14(3):033037, 2012.